Inorganic Chemistry

Article

pubs.acs.org/IC

Crystal Growth of New Hexahydroxometallates Using a Hydroflux

W. Michael Chance,[†] Daniel E. Bugaris,[†] Athena S. Sefat,[‡] and Hans-Conrad zur Loye*[,†]

[†]Department of Chemistry and Biochemistry, University of South Carolina, Columbia, South Carolina 29208, United States

[‡]Materials Science and Technology Division, Oak Ridge National Laboratory (ORNL), Oak Ridge, Tennessee 37831, United States

Supporting Information

ABSTRACT: A series of seven compounds, $Sr_2Mn(OH)_6$, $Ba_2Mn(OH)_6$, $Sr_2Co(OH)_6$, $Ba_2Co(OH)_6$, $Sr_2Ni(OH)_6$, $Ba_2Ni(OH)_6$, and $Ba_2Cu(OH)_6$, were synthesized using a low-melting hydroflux, a hybrid approach between aqueous hydrothermal and molten hydroxide flux techniques. Crystals of the hexahydroxometallates were obtained by dissolving appropriate amounts of alkaline-earth nitrates or hydroxides and transition-metal oxides, acetates, or chlorides in the hydroflux and reacting at 180−230 °C. The isostructural compounds all crystallize in the monoclinic space group $P2_1/n$. The monoclinic structure consists of isolated transition-metal octahedra within a three-dimensional framework of corner- and edge-shared eight-coordinate, alkaline-earth polyhedra. Magnetic susceptibility data show that all compounds are simple paramagnets. Thermogravimetric analysis indicates that these hydroxides lose water between 215 and 350 °C and transform into oxide products, the identity of which depends on the metal cations present in the parent hexahydroxometallates.

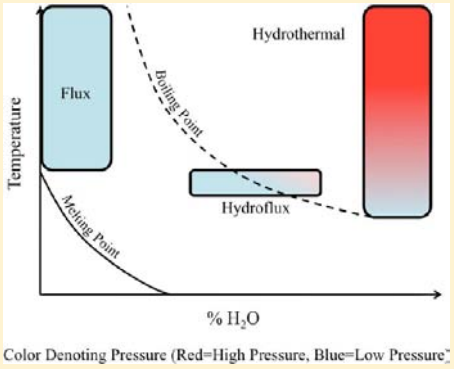

INTRODUCTION

Exploratory crystal growth continues to be one of the most effective approaches for investigating phase space and for identifying new compositions with novel structures and properties. The two most commonly used techniques for crystallizing solid-state inorganic materials rely on high-temperature solutions (fluxes) or hydrothermal (supercritical water) methods.[1] Because of the success of lower-temperature solvothermal and noncritical hydrothermal approaches for synthesizing organic−inorganic hybrids,[2−6] these methods have also been applied to the preparation of inorganic materials.[7−11] Among high-temperature fluxes, molten hydroxides are some of the best solvents for oxides and have been shown to be very effective for the growth of high-quality mixed-metal oxide single crystals.[12,13] In this paper, we describe the synthesis of new hexahydroxometallates using a low-temperature hydroflux, a hybrid approach between aqueous hydrothermal and molten hydroxide flux techniques. We have recently introduced this technique for the growth of single crystals of platinum group metal-containing hydroxides.[14]

Hydroxide fluxes are inorganic hydroxides, such as KOH or NaOH, that melt at conveniently low temperatures, 318 and 406 °C, respectively. Often eutectic mixtures of hydroxides, such as NaOH/KOH, are employed to reduce the melting point further. An alternative approach to lowering the melting point of hydroxides is to adjust the water content. Commercial hydroxides contain approximately 15 wt % water, which appreciably lowers the melting point versus the pure, anhydrous hydroxide. The intentional addition of extra water can further lower the melting point of hydroxide fluxes below 200 °C by forming a very low temperature melt and ultimately an aqueous solution. The term hydroflux has been suggested for the compositional regime where the melt has a very high water content yet is not an aqueous solution.[1] A hydroflux is thus best thought of as a combination of subcritical hydrothermal and flux techniques (Figure 1). In this compositional regime, a melt (hydroflux) forms at very low temperatures, making it possible to use simple poly(tetrafluoroethylene) (PTFE)-lined pressure vessels for containing the reaction. Little pressure is generated during the crystal growth process because water is solvated in the flux. The closed pressure vessels are needed only to seal the

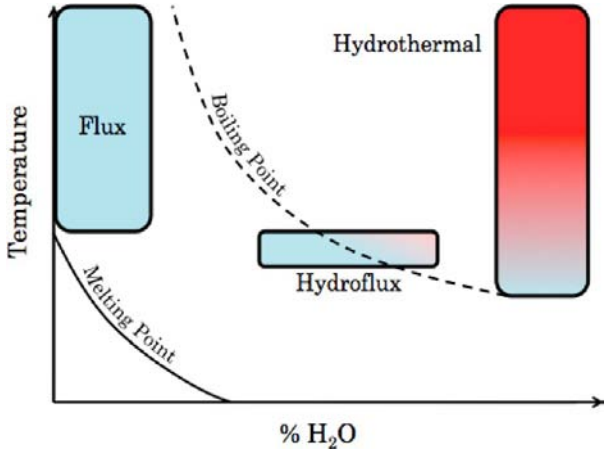

Figure 1. Comparison of hydrothermal, flux, and hydroflux techniques with respect to the temperature and water content. Red denotes a high vapor pressure, while blue denotes little to no vapor pressure.

Received: April 12, 2013
Published: October 9, 2013

   dx.doi.org/10.1021/ic400910g | *Inorg. Chem.* 2013, 52, 11723−11733

reaction to prevent dehydration, which would result in resolidification of the hydroxide and changes in the chemical properties of the flux during the course of the reaction.

Complex metal hydroxides, or hydroxometallates, are a relatively small class of inorganic compounds that were initially reported in the early 20th century[15−17] and usually consist of a combination of an electropositive alkali or alkaline-earth metal and a first-row transition metal or a main-group metal. Examples of these materials include the silicon-free hydrogarnets[18,19] and hexahydroxometallates,[20−25] which include the well-explored hydroxystannates.[26−35] Although hydroxometallates have been known for a relatively long time, the lack of high-quality crystals has precluded extensive structural characterization in many instances. Their thermal behavior, investigated in some cases by thermogravimetric analysis (TGA), has been reported to often follow a general reaction scheme (eq 1), which consists of dehydration and formation of an oxide product.

$$A_xB_y(OH)_z \rightarrow A_xB_yO_{z/2} + \frac{z}{2}H_2O \quad (1)$$

On the basis of this reaction scheme, hydroxometallates can be used as precursors to explore the low-temperature formation of oxides and the potential discovery of new low-temperature ternary or (if starting with more complex hydroxometallates) quaternary or even higher mixed-metal oxides.

Herein we report the synthesis, structure, and magnetic characterization of a series of novel mixed-metal hexahydroxometallates $A_2B(OH)_6$ (A = Sr, Ba; B = Mn, Ni, Co, Cu). In addition, the suitability of these hexahydroxometallates to function as precursors for the synthesis of oxides was investigated and is detailed within.

EXPERIMENTAL METHODS

Reagents. The following reagents were used as obtained: KOH (Fisher Scientific, ACS-grade pellets), NaOH (Fisher Scientific, ACS-grade pellets), $Sr(OH)_2·8H_2O$ (Alfa Aesar, 99%), $Sr(NO_3)_2$ (Fisher Scientific, ACS grade), $Ba(OH)_2·8H_2O$ (Alfa Aesar, 99%), $Ba(NO_3)_2$ (Alfa Aesar, 99.95%), $MnCl_2·4H_2O$ (Alfa Aesar, 97%), $CoCl_2·6H_2O$ (B&A Chemicals, ACS grade), $Ni(NO_3)_2·6H_2O$ (Alfa Aesar, technical grade), and CuO (Alfa Aesar, 99.5%).

Crystal Growth. All products were synthesized in 23 mL PTFE-lined stainless steel autoclaves. A typical synthesis involved reacting approximately 8−12 g of alkali-metal hydroxide(s), stoichiometric quantities of alkaline-earth and transition-metal precursors, and 6−8 g of water at 180−230 °C for 12−24 h. Alkaline-earth precursors investigated include chlorides, hydroxides, and nitrates. The transition-metal precursor selection profoundly impacted the phase purity and crystal quality. Transition-metal precursors investigated included acetates, chlorides, nitrates, and oxides. For each individual composition, the optimal precursors varied.

$Sr_2Mn(OH)_6$ and $Ba_2Mn(OH)_6$. A total of 2 mmol of $Sr(OH)_2·8H_2O$ or $Ba(OH)_2·8H_2O$ and 1 mmol of $MnCl_2·4H_2O$ were added to a hydroflux consisting of 0.11 mol of KOH, 0.1 mol of NaOH, and 0.33 mol of distilled water. This mixture was heated to 230 °C at a rate of 5 °C/min and held for 24 h before being cooled at a rate of 0.2 °C/min to 80 °C.

$Sr_2Co(OH)_6$ and $Ba_2Co(OH)_6$. A total of 1.5 mmol of $Sr(OH)_2·8H_2O$ or $Ba(OH)_2·8H_2O$ and 1 mmol of $CoCl_2·6H_2O$ were added to a hydroflux consisting of 0.11 mol of KOH, 0.1 mol of NaOH, and 0.33 mol of distilled water. This mixture was heated to 230 °C at a rate of 5 °C/min and held for 24 h before being cooled at a rate of 0.2 °C/min to 80 °C.

$Sr_2Ni(OH)_6$ and $Ba_2Ni(OH)_6$. A total of 2 mmol of $Sr(NO_3)_2$ or $Ba(NO_3)_2$ and 1 mmol of $Ni(NO_3)_2·6H_2O$ were added to a hydroflux consisting of 0.23 mol of KOH and 0.33 mol of distilled water. This mixture was heated to 180 °C for the strontium analogue and 200 °C for the barium analogue at a rate of 5 °C/min and held for 24 h before being cooled at a rate of 0.3 °C/min to 80 °C.

$Ba_2Cu(OH)_6$. A total of 2 mmol of $Ba(OH)_2·8H_2O$ and 1 mmol of CuO were added to a hydroflux consisting of 0.11 mol of KOH, 0.1 mol of NaOH, and 0.33 mol of distilled water. This mixture was heated to 230 °C at a rate of 5 °C/min and held for 24 h before being cooled at a rate of 0.2 °C/min to 80 °C.

The ranges of reaction conditions that yielded the desired hydroxides are detailed in Table 1. The resulting hydroxides were sonicated in methanol and collected by vacuum filtration. Because of the presence of carbonate impurities in the alkali-metal hydroxides and the propensity of alkaline media to sequester carbon dioxide, crystals of alkaline-earth carbonates readily form during the course of these reactions. These crystals of barium and strontium carbonate are often large (approximately 0.5−1 cm) and can be removed by mechanical separation.

To inhibit the formation of carbonates, a number of experimental strategies were investigated. Sealing the reactions in an inert atmosphere (N_2) did not prevent the formation of carbonate byproducts. This may be due to either the natural propensity for NaOH and KOH to sequester CO_2 from the atmosphere or the tendency for fluoropolymers to become permeable to gas exchange at elevated temperatures.[36,37] To eliminate the alkali hydroxides as a possible carbonate source, experiments with K_2O and Na_2O/Na_2O_2 as precursors were carried out, but the products of these reactions vastly differed from those involving hydroxide precursors. Pretreatment of the hydroflux with barium or strontium salts followed by filtration of the formed carbonates yielded inconsistent results. Investigations into the possibility of an alkaline-earth hydroflux yielded only modest amounts of hexahydroxometallates with significant transition-metal hydroxide and amorphous byproducts. The most promising method of eliminating carbonate formation was the introduction of a mineralizer. In the preparation of strontium hexahydroxometallates, WO_3 inhibits the formation of carbonates completely and also promotes crystal growth along specific directions for each system, resulting in significantly elongated crystals (Figure 2).

Scanning Electron Microscopy (SEM). Single crystals were analyzed via SEM with an FEI Quanta scanning electron microscope operating in low-vacuum mode. Energy-dispersive spectroscopy verified the presence and approximate ratios of the metals in each compound.

IR Spectroscopy. IR spectra were recorded with a Perkin-Elmer Spectrum 100 FT-IR spectrometer. All samples were ground to a powder using an agate mortar and pestle, and four scans ranging from 4500 to 600 cm^{-1} were averaged.

TGA. All compounds were heated under flowing air or nitrogen at a rate of 100 mL/min in a TA Instruments SDT Q600 analyzer with an alumina pan as the sample container. Samples were heated at a rate of 10 °C/min to 1000−1200 °C.

Powder X-ray Diffraction. Phase identification/purity was determined by powder X-ray diffraction using either a Rigaku DMAX-2100 or a Rigaku Ultima IV powder X-ray diffractometer with Cu Kα radiation (λ = 1.5418 Å). Samples were ground to a fine powder, and data were collected from 2θ = 10 to 80° with a step size of 0.04°.

Magnetic Measurements. The magnetic susceptibilities of $Sr_2Mn(OH)_6$, $Ba_2Mn(OH)_6$, $Sr_2Co(OH)_6$, $Ba_2Co(OH)_6$, $Sr_2Ni(OH)_6$, and $Ba_2Ni(OH)_6$ were measured as a function of the temperature using a Quantum Design MPMS SQUID magnetometer. The polycrystalline samples were placed in a gelatin capsule. For a typical temperature sweep experiment, the sample was first cooled to 5 K under zero-field-cooled (zfc) conditions and data were collected upon warming to 300 K in an applied field of 1000 Oe. Then the sample was field-cooled (fc) to 5 K from room temperature in 1000 Oe while data were collected.

Structure Determination. Single-crystal X-ray diffraction data were collected at 298 K on a Bruker SMART APEX CCD diffractometer (Mo Kα radiation, λ = 0.71073 Å). The crystal-to-detector distance was 5.048 cm. Crystal decay was monitored by

dx.doi.org/10.1021/ic400910g | Inorg. Chem. 2013, 52, 11723−11733

Table 1. Range of Working Reaction Conditions for the Synthesis of Hexahydroxometallates via the Hydroflux Method

product	temperature profile	hydroflux composition	alkaline-earth precursor	transition-metal precursor	yield (%)
$Sr_2Mn(OH)_6$	ramp 5 °C/min to 200–230 °C, hold 12–24 h, cool to 80 °C at 1–0.1 °C/min	0.2–0.25 mol of KOH/NaOH (53:47) or KOH and 0.3–0.4 mol of H_2O	2 mol of $Sr(OH)_2{\cdot}8H_2O$ or $Sr(NO_3)_2$	1 mmol of $MnCl_2{\cdot}4H_2O$	87
$Sr_2Co(OH)_6$	ramp 5 °C/min to 200–230 °C, hold 12–24 h, cool to 80 °C at 1–0.1 °C/min	0.2–0.25 mol of KOH/NaOH (53:47) or KOH and 0.3–0.4 mol of H_2O	1.5 mmol of $Sr(OH)_2{\cdot}8H_2O$ or $Sr(NO_3)_2$	1 mmol of $CoCl_2{\cdot}6H_2O$	75
$Sr_2Ni(OH)_6$	ramp 5 °C/min to 180–230 °C, hold 12–36 h, cool to 80 °C at 1–0.1 °C/min	0.2–0.25 mol of KOH and 0.3–0.4 mol of H_2O	2 mmol of $Sr(NO_3)_2$	1 mmol of $Ni(NO_3)_2{\cdot}6H_2O$	93
$Ba_2Mn(OH)_6$	ramp 5 °C/min to 200–230 °C, hold 12–24 h, cool to 80 °C at 1–0.1 °C/min	0.2–0.25 mol of KOH/NaOH (53:47) or KOH and 0.3–0.4 mol of H_2O	2 mmol of $Ba(OH)_2{\cdot}8H_2O$ or $Ba(NO_3)_2$	1 mmol of $MnCl_2{\cdot}4H_2O$	85
$Ba_2Co(OH)_6$	ramp 5 °C/min to 200–230 °C, hold 12–24 h, cool to 80 °C at 1–0.1 °C/min	0.2–0.25 mol of KOH/NaOH (53:47) or KOH and 0.3–0.4 mol of H_2O	1.5 mmol of $Ba(OH)_2{\cdot}8H_2O$ or $Ba(NO_3)_2$	1 mmol of $CoCl_2{\cdot}6H_2O$	75
$Ba_2Ni(OH)_6$	ramp 5 °C/min to 180–230 °C, hold 12–36 h, cool to 80 °C at 1–0.1 °C/min	0.2–0.25 mol of KOH and 0.3–0.4 mol of H_2O	2 mmol of $Ba(NO_3)_2$	1 mmol of $Ni(NO_3)_2{\cdot}6H_2O$	93
$Ba_2Cu(OH)_6$	ramp 5 °C/min to 200–230 °C, hold 12–24 h, cool to 80 °C at 1–0.1 °C/min	0.2–0.25 mol of KOH/NaOH (53:47) or KOH and 0.3–0.4 mol of H_2O	2 mmol of $Ba(OH)_2{\cdot}8H_2O$ or $Ba(NO_3)_2$	1 mmol of CuO	90

recollecting the initial 50 frames at the end of the data collection process. Data were collected by a scan of 0.3° in ω in groups of 606 frames at ϕ settings of 0°, 90°, 180°, and 270°. The exposure time was 20 s/frame. The collection of the intensity data was carried out with the program *SMART*.[38,39] Cell refinement and data reduction were carried out using the program *SAINT+*.[38,39] A numerical absorption correction was performed with use of the program *SADABS*.[38,39] The program *SADABS* was also employed to make incident beam and decay corrections. The structure was solved with the direct methods program *SHELXS* and refined with the full-matrix least-squares program *SHELXTL*.[40] After H atoms were located by difference Fourier syntheses, O–H bond lengths were restrained to d = 0.85(2) Å using the DFIX command. Final refinements included anisotropic displacement parameters for the metal and O atoms and isotropic displacement parameters for the H atoms. In all structures, restrained refinement of the H-atom parameters resulted in physically reasonable displacement parameters (similar in magnitude to the parent O atoms) and no unacceptably short interatomic contact distances, providing strong support for the reported positions. A secondary extinction correction was also applied. Additional experimental details are given in Table 2 and the Supporting Information. Selected metrical details are presented in Table 3.

RESULTS AND DISCUSSION

Synthesis. Single crystals of the hexahydroxometallates, $Sr_2Mn(OH)_6$, $Ba_2Mn(OH)_6$, $Sr_2Co(OH)_6$, $Ba_2Co(OH)_6$, $Sr_2Ni(OH)_6$, $Ba_2Ni(OH)_6$, and $Ba_2Cu(OH)_6$, were grown from a hydroflux (Figure 3) using the conditions listed in Table 1. Crystals of $BaCO_3$ or $SrCO_3$ tended to form as a secondary phase because of the presence of sodium and potassium carbonate in the hydroxide reagent along with carbon dioxide sequestered from the surrounding atmosphere. Close to single-phase samples could be obtained by separating the carbonate crystals from the hexahydroxometallate crystals with a sieve. Strontium carbonate could be eliminated from the strontium hexahydroxometallates with the addition of WO_3 as a mineralizer, but when used with the barium analogues, ternary and quaternary oxide byproducts were formed.

The nature of the reagents and the quantities of the different hydroxides used had a significant influence on the degree of crystallinity and identity of the products that were isolated from the reaction mixture. For example, the synthesis of both $Sr_2Mn(OH)_6$ and $Ba_2Mn(OH)_6$ worked best if $MnCl_2{\cdot}4H_2O$ was used as the manganese source instead of $Mn(CH_3COO)_2$ for crystal growth because the use of $Mn(CH_3COO)_2$ resulted in the formation of microcrystalline powders of $SrMnO_3$ as a secondary phase. Also, using larger ratios of NaOH/KOH to the alkaline-earth metals and transition metals led to the formation of $NaMnO_2$ and $BaMnO_3$ rather than single crystals of $Sr_2Mn(OH)_6$ and $Ba_2Mn(OH)_6$. For the cobalt-containing phases, $CoCl_2{\cdot}6H_2O$ was found to be the superior starting material over the oxides Co_3O_4 and Co_2O_3 and $Co(NO_3)_2{\cdot}6H_2O$, although all yielded the hydroxometallates, albeit in lesser yield. Single-phase hydroxocobaltates were only obtained when using $CoCl_2{\cdot}6H_2O$ as the cobalt source. Interestingly, while the above syntheses of the manganese- and cobalt-containing hexahydroxometallates worked when using either NaOH, KOH, or a eutectic mixture of the two as the hydroflux, the synthesis of $Sr_2Ni(OH)_6$ and $Ba_2Ni(OH)_6$ succeeded only in a KOH-based hydroflux, with crystallization optimized at lower operating temperatures of 180 and 200 °C, respectively.

While it is apparent that the different precursors used influenced the reaction outcome, it is difficult to explain fully why specific conditions and reagents led to specific outcomes. Nonetheless, observations during experimentation do show

dx.doi.org/10.1021/ic400910g | Inorg. Chem. 2013, 52, 11723–11733

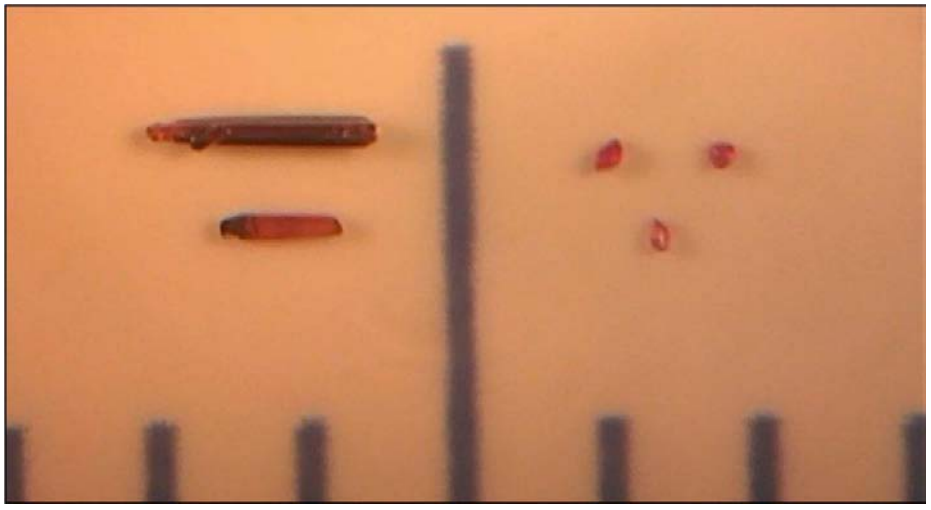

Figure 2. $Sr_2Co(OH)_6$ crystals grown in the presence of a WO_3 mineralizer (left) exhibiting a different crystal morphology and increased size compared with crystals grown without WO_3 (right). Graduations are in millimeters.

some definite trends. The use of metal chloride or metal nitrate salts, in general, resulted in improved crystallization of the hydroxometallates compared to the use of metal oxides or metal organic salts (acetate, acetylacetonate, oxalate, etc.). In addition, the metal oxidation state in the starting reagent, more than anything, affected the specific product(s) obtained as well as the relative ratio of the products when more than one phase crystallized. These results are consistent with what has been observed for the crystallization of platinum metal hydroxometallates,[14] where reagents such as $H_2[PtCl_6]$, $Pd(NH_3)_2Cl_2$, and K_2PdCl_6 resulted in the formation of numerous compositions.

The hydroflux itself, a combination of water with NaOH, KOH, or a mixture of NaOH and KOH, acting as the solvent for crystal growth, appeared to have only a small influence on the reaction outcome. However, the addition of barium and strontium hydroxides to the hydroflux created a more reactive reaction environment, no doubt aided by the presence of large divalent cations that are readily incorporated into the product structures. One might anticipate that expanding this line of research to include other large di- or trivalent cations will likely be successful.

Structures. All members of this series were solved in the space group $P2_1/n$ of the monoclinic crystal system. The structures of the zinc and copper members have been described in the literature as analogues of the Li_2O structure.[25] $Ba_2Cu(OH)_6$ was reported previously in the alternate setting $P2_1/c$[20] but has been included in this investigation in order to normalize the series. In each instance, the alkaline-earth element coordinates to eight O atoms in what can be described as either a highly distorted square antiprism or a distorted bicapped trigonal prism. These polyhedra are corner- and edge-shared to form a three-dimensional framework. All transition metals are octahedrally coordinated by oxygen, where the octahedra are isolated from each other. These octahedra are framed by eight alkaline-earth polyhedra (Figures 4 and 5). Two formula units are contained in each unit cell (Figure 6).

As expected, the average transition-metal-to-oxygen bond length decreases across the period from manganese to nickel for both the strontium and barium analogues (Table 3). The barium hexahydroxocuprate is an exception in that the copper is in a distorted octahedral coordination environment because of a Jahn–Teller distortion. The average alkaline-earth-metal-to-oxygen bond lengths differ between the strontium and barium analogues, with the barium compounds having slightly longer bonds by 0.153–0.193 Å, as expected given the larger size of barium. The smallest difference in the bond lengths was observed for the nickel analogues, and the greatest difference was observed for the manganese analogues. Within the strontium series, the strontium bond distance with oxygen is essentially constant [2.642(1)–2.640(1) Å]. However, the barium analogues appear to exhibit a slight contraction in the barium-to-oxygen bond distances across the period [2.824(1)–2.794(1) Å], with the copper analogue again being an exception.

IR Spectroscopy. As shown in Figures 7 and S1–S6 in the Supporting Information, the spectra of all of the hexahydroxometallates have two broad absorption bands in the 3400–3600 cm^{-1} range, consistent with the presence of hydroxyl groups in the structure. Each hexahydroxometallate structure has three unique hydroxide groups that are hydrogen-bonded, broadening the bands.

Bond Valence Sum (BVS) Analysis. The BVS analysis results listed in Table 4 were obtained using parameters by Brown.[41] The BVSs are all close to what is expected (A, +2; B, +2; OH, −1), confirming the divalent oxidation states of the metals. Sutovic et al. reported similar BVS results in the reinvestigation of $Sr_2Cu(OH)_6$.[42]

TGA. It is well-known that mixed-metal hydroxides, oxalates, nitrates, and acetates can be used as precursors in the preparation of interesting oxides.[43] Often, solid solutions or mixtures of two separate hydroxides have been prepared and then converted into the corresponding oxide. There are a number of instances where this technique of precipitation of a mixed hydroxide product has been used to form perovskites. For example, Vidysagar et al. synthesized solid solutions of composition $Ln_{1-x}M_x(OH)_3$ (Ln = La, Nd; M = Cr, Fe) with metal nitrate solutions and NaOH and generated the corresponding perovskite products at low temperature.[44] A number of iridium and osmium perovskites were synthesized in a similar manner by Sarkozy et al.[45,46] Less often have *crystallized* hydroxides been studied for their oxide thermal conversion products. Morán-Miguélez and colleagues studied crystallization of the so-called silicon-free hydrogarnets with

dx.doi.org/10.1021/ic400910g | *Inorg. Chem.* 2013, 52, 11723–11733

Table 2. Crystallographic Data for $A_2B(OH)_6$ (A = Sr, Ba; B = Mn, Co, Ni, Cu)[a]

compound	$Sr_2Mn(OH)_6$	$Sr_2Co(OH)_6$	$Sr_2Ni(OH)_6$	$Ba_2Mn(OH)_6$	$Ba_2Co(OH)_6$	$Ba_2Ni(OH)_6$	$Ba_2Cu(OH)_6$
fw (g/mol)	332.23	336.22	336.00	431.67	435.66	435.44	440.27
color and habit	brown, prism	pink, prism	green, prism	brown, prism	pink, prism	green, prism	blue, prism
a (Å)	5.801(1)	5.764(1)	5.762(1)	6.154(1)	6.085(1)	6.0840(12)	6.034(1)
b (Å)	6.132(1)	6.135(1)	6.129(1)	6.333(1)	6.227(1)	6.1806(12)	6.438(1)
c (Å)	8.139(2)	8.097(2)	8.080(2)	8.548(2)	8.495(2)	8.4429(17)	8.384(2)
β (deg)	91.14(3)	90.80(3)	90.73(3)	90.86(3)	90.69(3)	90.68(3)	92.51(3)
V (Å^3)	289.5(1)	286.3(1)	285.3(1)	333.1(1)	321.8(1)	317.45(1)	325.4(1)
ρ_c (g/cm^3)	3.812	3.900	3.911	4.304	4.496	4.555	4.493
μ (mm^{-1})	20.465	21.383	21.849	13.521	14.609	15.164	15.167
$F(000)$	310	314	316	382	386	388	390
cryst size (mm^3)	0.200 × 0.088 × 0.070	0.064 × 0.062 × 0.058	0.100 × 0.058 × 0.054	0.114 × 0.096 × 0.076	0.082 × 0.062 × 0.040	0.053 × 0.050 × 0.042	0.090 × 0.082 × 0.056
θ_{max} (deg)	32.17	32.12	31.91	32.05	31.78	28.28	31.96
index ranges	$-8 \le h \le 8$; $-9 \le k \le 9$; $-12 \le l \le 12$	$-8 \le h \le 8$; $-8 \le h \le 8$; $-11 \le l \le 12$	$-8 \le k \le 8$; $-9 \le k \le 9$; $-11 \le l \le 11$	$-9 \le h \le 9$; $-9 \le k \le 9$; $-12 \le l \le 12$	$-8 \le h \le 8$; $-9 \le k \le 9$; $-12 \le l \le 12$	$-8 \le h \le 8$; $-9 \le k \le 8$; $-11 \le l \le 11$	$-8 \le h \le 8$; $-9 \le k \le 9$; $-12 \le l \le 12$
reflns collected	4753	4539	4595	5042	5155	4136	5246
indep reflns	1000	943	956	1102	1079	786	1097
GOF on F^2	1.149	1.182	1.143	1.180	1.115	1.037	1.105
R indices (all data)	R1 = 0.0183, wR2 = 0.0485	R1 = 0.0160, wR2 = 0.0328	R1 = 0.0151, wR2 = 0.0317	R1 = 0.0143, wR2 = 0.0335	R1 = 0.0126, wR2 = 0.0304	R1 = 0.0157, wR2 = 0.0338	R1 = 0.0141, wR2 = 0.0333
largest peak/ diffraction hole (e/ Å^3)	0.876/−0.725	0.517/−0.523	0.376/−0.538	0.617/−0.908	1.105/−0.692	1.193/−1.254	0.537/−1.184

[a]For all structures, T = 298(2) K, λ = 0.71073 Å, the space group is $P2_1/n$, and Z = 2.

dx.doi.org/10.1021/ic400910g | Inorg. Chem. 2013, 52, 11723−11733

Table 3. Selected Bond Distances (Å) and Angles (deg) for $A_2B(OH)_6$ (A = Sr, Ba; B = Mn, Co, Ni, Cu)

	$Sr_2Mn(OH)_6$	$Sr_2Co(OH)_6$	$Sr_2Ni(OH)_6$	$Ba_2Mn(OH)_6$	$Ba_2Co(OH)_6$	$Ba_2Ni(OH)_6$	$Ba_2Cu(OH)_6$
A–O3	2.478(2)	2.490(2)	2.500(1)	2.671(2)	2.661(2)	2.657(2)	2.641(2)
A–O2	2.494(2)	2.519(2)	2.531(1)	2.705(2)	2.710(2)	2.704(2)	2.715(2)
A–O1	2.506(2)	2.526(2)	2.534(2)	2.701(2)	2.687(1)	2.679(2)	2.732(2)
A–O1	2.539(2)	2.547(2)	2.550(2)	2.760(2)	2.751(1)	2.738(2)	2.748(2)
A–O3	2.642(2)	2.643(2)	2.639(2)	2.848(2)	2.832(2)	2.809(2)	2.831(2)
A–O2	2.681(2)	2.689(2)	2.687(2)	2.920(2)	2.905(2)	2.883(2)	2.923(2)
A–O3	2.873(2)	2.851(2)	2.840(2)	2.998(2)	2.965(2)	2.951(2)	2.946(2)
A–O2	2.923(2)	2.858(2)	2.841(2)	2.985(2)	2.938(2)	2.928(2)	2.930(2)
B–O2 (×2)	2.097(2)	2.055(2)	2.039(1)	2.150(2)	2.085(1)	2.065(2)	1.969(2)
B–O1 (×2)	2.166(2)	2.104(2)	2.084(1)	2.193(2)	2.114(2)	2.098(2)	1.955(2)
B–O3 (×2)	2.256(2)	2.224(2)	2.191(1)	2.315(2)	2.252(2)	2.197(2)	2.804(2)
O1–B–O1	180.0	180.0	180.00(8)	180.0	180.0	180.00(13)	180.0
O1–B–O2	89.09(6)	89.14(6)	89.34(6)	89.79(7)	89.76(6)	89.37(9)	88.75(7)
O1–B–O3	89.05(6)	89.64(6)	89.97(6)	89.38(6)	89.95(6)	89.71(9)	88.49(6)
O2–B–O2	180.0	180.0	180.0	180.0	180.0	179.999(1)	180.0
O2–B–O3	88.70(6)	87.92(6)	87.87(6)	89.15(6)	89.28(6)	89.60(9)	86.88(6)
O3–B–O3	180.0	180.0	180.0	180.00(8)	180.0	180.00(7)	180.0

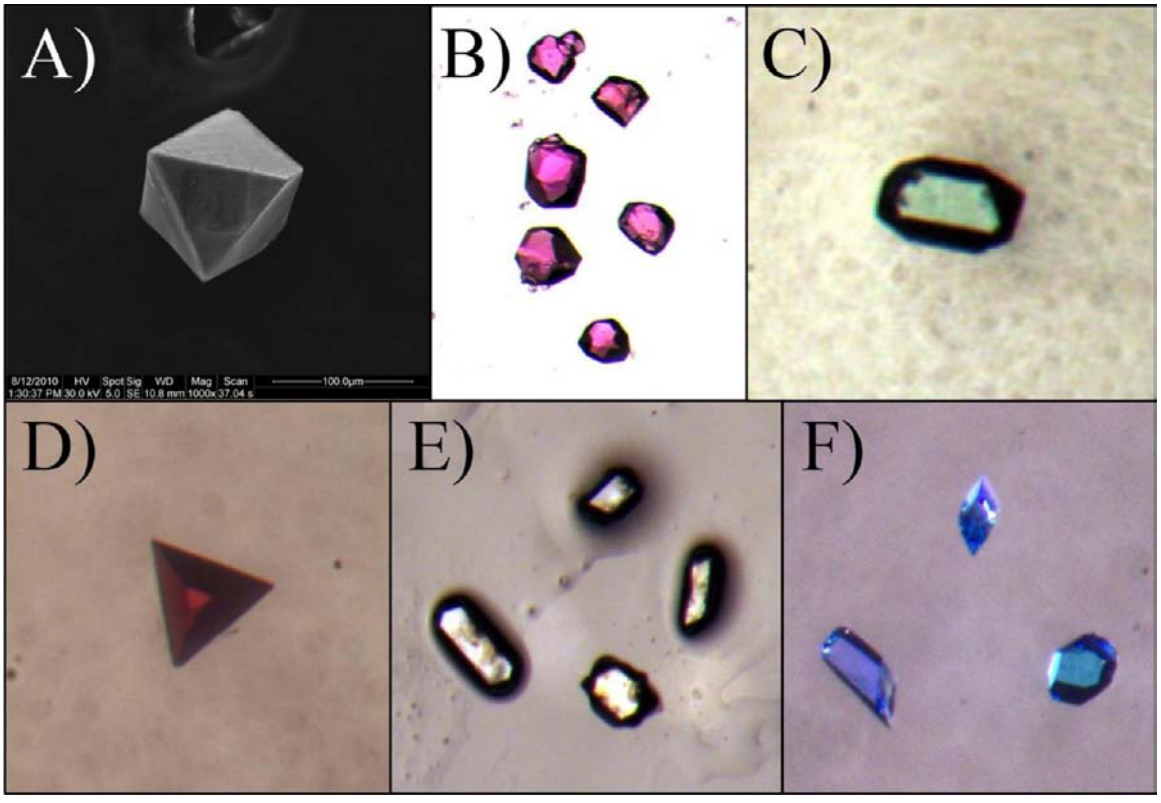

Figure 3. SEM image of (a) $Sr_2Mn(OH)_6$ and optical images of (b) $Sr_2Co(OH)_6$, (c) $Sr_2Ni(OH)_6$, (d) $Ba_2Mn(OH)_6$, (e) $Ba_2Co(OH)_6$, and (f) $Ba_2Cu(OH)_6$.

composition $A_3B_2(OH)_{12}$.[19] They reported that the thermal conversion mechanism proceeds by the general reaction given in eq 2.

$$A_3B_2(OH)_{12} \rightarrow A_3B_2O_6 + 6H_2O\ (T = 1000\ ^\circ C) \qquad (2)$$

Similarly, Li and co-workers reported details about the thermal behavior of the chromium, iron, and aluminum hydrogarnets of strontium.[47] Their analysis concluded that for these hydroxides a loss of four water molecules occurred between 260 and 330 °C. One interesting finding was that $Sr_3Al_2O_6$ was readily produced at temperatures of only 600 °C, compared with 1600 °C reported for a traditional solid-state reaction.[48] It is, of course, also possible for some reactions to phase-separate and generate mixed-phase products, as was observed for thermal decomposition of $Sr_3Cr_2(OH)_{12}$ into SrO and $SrCrO_4$.

$Sr_2Cu(OH)_6$, a previously reported structural analogue of the title series, was utilized by Shimakawa and colleagues as a single-source precursor for the preparation of Sr_2CuO_{3+x}, a phase that can be superconducting under certain processing

dx.doi.org/10.1021/ic400910g | Inorg. Chem. 2013, 52, 11723–11733

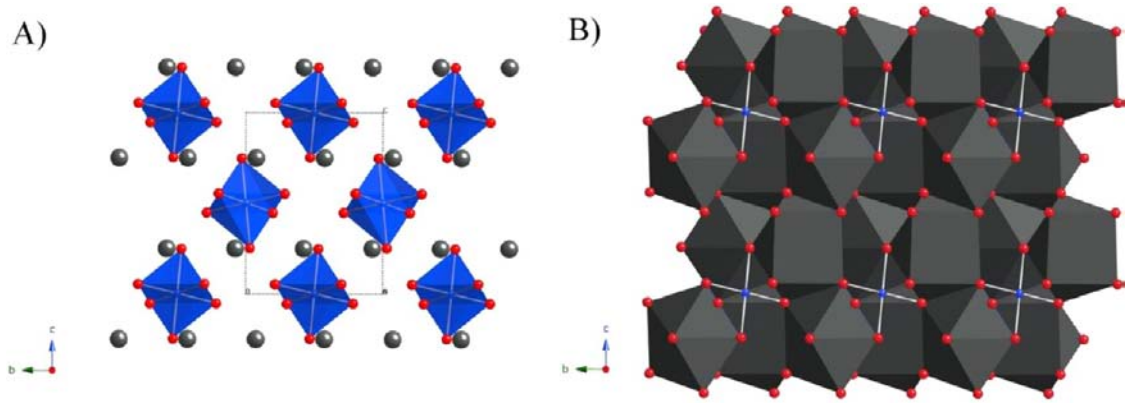

Figure 4. Extended structure of $Sr_2Co(OH)_6$ with the cobalt octahedra featured in blue and Sr atoms shown in gray (a) and with the strontium polyhedra shown in gray with the cobalt coordination in blue (b). O atoms are shown in red, and H atoms are omitted for clarity.

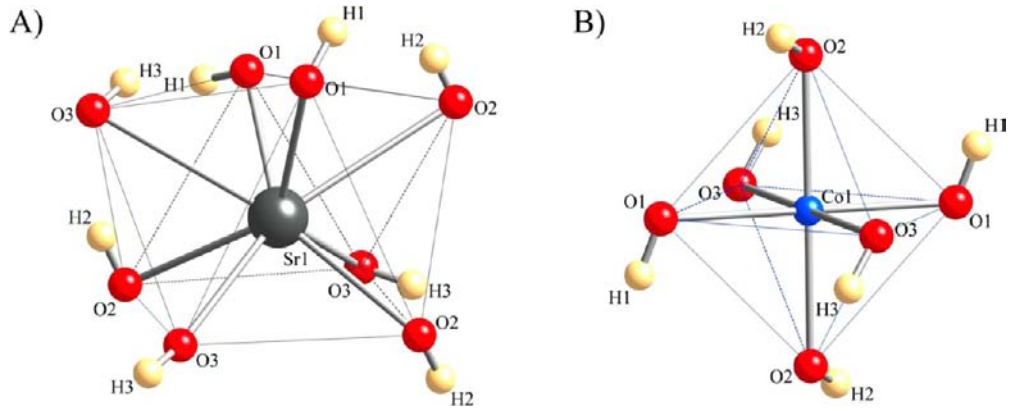

Figure 5. Local coordination environments of the Sr (a) and Co (b) atoms.

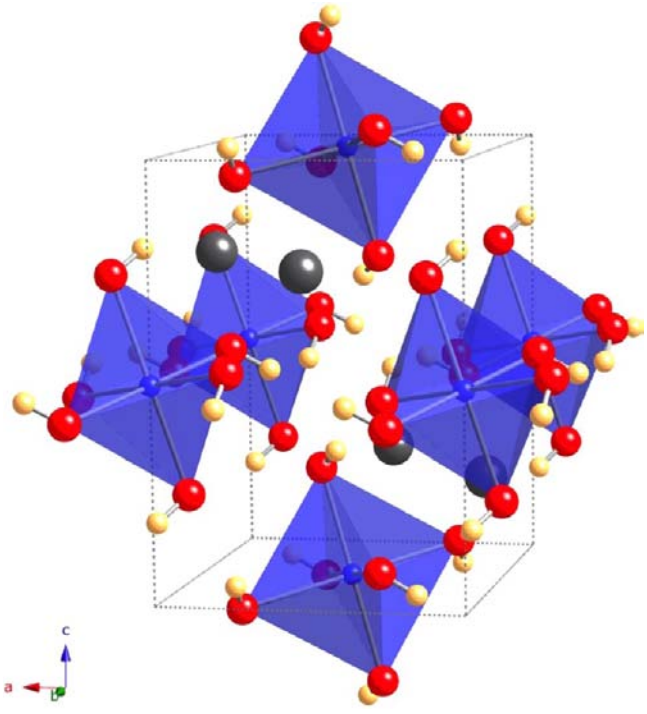

Figure 6. Unit cell of $Sr_2Co(OH)_6$ with Sr atoms in gray, Co in blue with its coordination polyhedra in blue, O in red, and H in light orange.

conditions.[49] Nagai and co-workers used calcium-substituted $Sr_2Cu(OH)_4{\cdot}H_2O$ and barium-substituted $Sr_2Cu(OH)_6{\cdot}H_2O$ prepared as powders by the method introduced by Scholder and Schwochow as precursors for oxides in the (Ba, Sr, Ca)−Cu−O system.[50,51] Such reactions demonstrate the utility of using hydroxometallates as precursors to overcome diffusion barriers, allowing reactions to be carried out at lower temperatures. The low reaction temperatures can possibly lead to the isolation of new, metastable materials. To learn more about mixed-metal hydroxides as potential oxide precursors, where the precise atomic ratio coupled with atomic level mixing to minimize cation diffusion should prove beneficial, we studied the thermal decomposition behavior of this series of isostructural hexahydroxometallates.

TGA of the new hexahydroxometallates was performed in air and nitrogen, and the decomposition products are given in Table 5. A careful analysis of the powder X-ray diffraction patterns collected on samples isolated at each temperature where a plateau was evident in the data indicates that the hexahydroxometallates dissociate into alkaline-earth hydroxides and transition-metal-containing products, except for $Sr_2Mn(OH)_6$. All of the hexahydroxometallates studied show a first weight loss between 210 and 350 °C in air, which corresponds to the breakdown of the hydroxide lattice, yielding corresponding oxides at higher temperature (Figures 8 and S7−S17 in the Supporting Information). The stoichiometry of the final products is dependent upon the metal identities and does not follow a general reaction scheme.

dx.doi.org/10.1021/ic400910g | *Inorg. Chem.* 2013, 52, 11723−11733

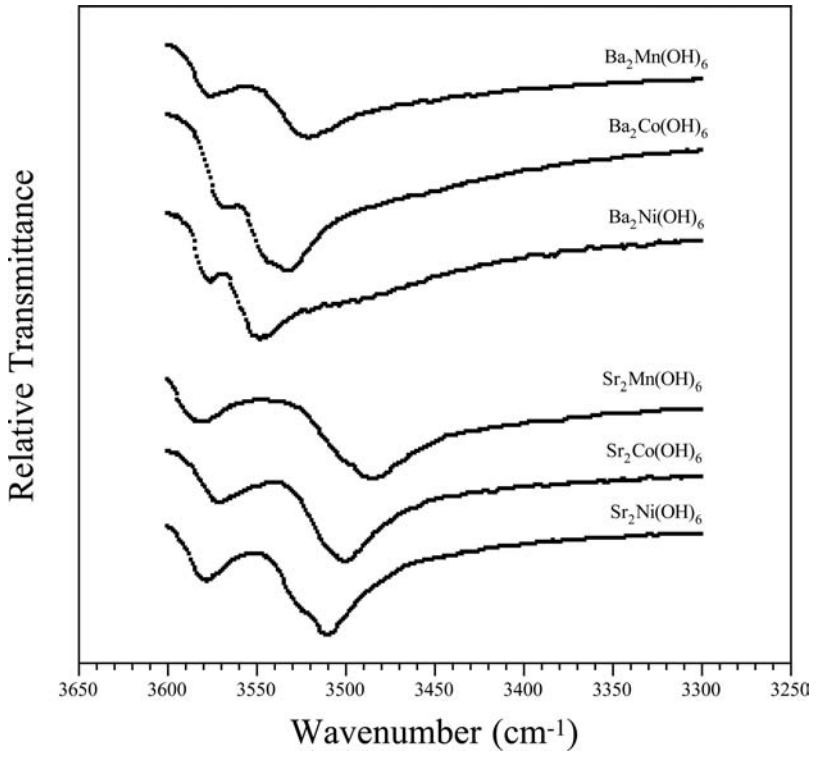

Figure 7. IR absorption spectra for selected hydroxides from 3650 to 3250 cm^{-1}.

Table 4. Calculated BVSs for the Synthesized Compounds

	$A_2B(OH)_6$						
	$Sr_2Mn(OH)_6$	$Sr_2Co(OH)_6$	$Sr_2Ni(OH)_6$	$Ba_2Mn(OH)_6$	$Ba_2Co(OH)_6$	$Ba_2Ni(OH)_6$	$Ba_2Cu(OH)_6$
A	2.12	2.08	2.06	1.97	2.05	2.11	2.03
B	2.16	1.85	1.91	1.91	1.74	1.82	1.96
O1	1.03	0.97	0.97	0.94	0.93	0.94	1.06
O2	1.13	1.06	1.06	1.03	1.01	1.06	1.12
O3	1.03	0.98	0.99	0.96	0.97	1.03	0.83

Table 5. Decomposition Products of the Hexahydroxometallates in Air and Nitrogen As Determined by Powder X-ray Diffraction

hydroxometallate	decomposition product(s)	temperature (°C)
$Sr_2Mn(OH)_6$	air−$Sr_2MnO_{4-\delta}$	900
	N_2−$Sr_2MnO_{4-\delta}$	900
$Sr_2Co(OH)_6$	air−$Sr_6Co_5O_{15}$ + $SrCO_3$	420
	N_2−$Sr(OH)_2$ + unidentified products	800
$Sr_2Ni(OH)_6$	air−$Sr_9Ni_{6.61}O_{21}$ + $SrCO_3$	815
	N_2−$Sr_2Ni_2O_{5\pm\delta}$ + $Sr(OH)_2$	375
$Ba_2Mn(OH)_6$	air−$Ba_3Mn_2O_8$ + $BaMnO_3$	710
	N_2−$BaMnO_{3-x}$ + $BaCO_3$	800
$Ba_2Co(OH)_6$	air−$Ba_3Co_2O_6(CO_3)_{0.6}$ + $BaCO_3$	525
	N_2−Ba_2CoO_4	900
$Ba_2Ni(OH)_6$	air−$BaNi_{0.83}O_{2.5\pm\delta}$ + $BaCO_3$	1100
	N_2−$BaNiO_3$ + $BaCO_3$	325

Thermal decomposition of $Sr_2Mn(OH)_6$ under an inert atmosphere occurs in four steps (Figure 9). The first weight loss is observed by 260 °C with a product of $Sr_2MnO_4(OH)$.[52] A very small weight loss is seen around 400 °C followed by another small weight loss around 640 °C. Varying amounts of both $Sr_2MnO_4(OH)$ and Sr_2MnO_4[53] are present during these

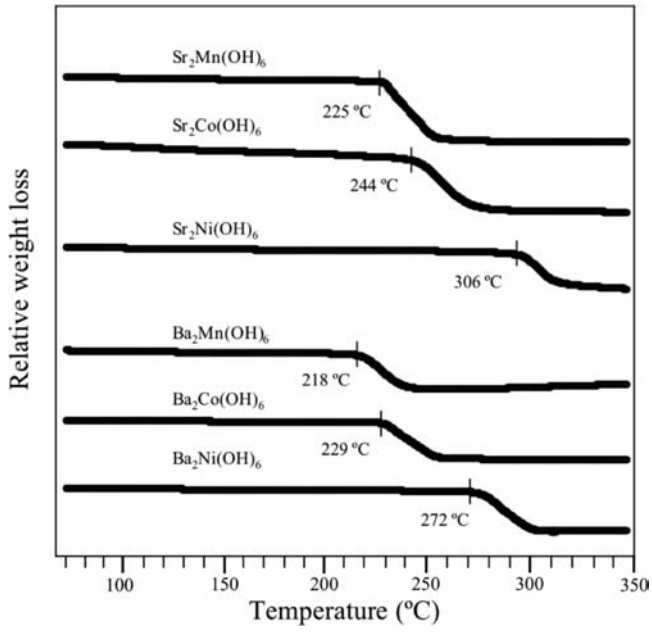

Figure 8. TGA data for selected hydroxides in air. Temperatures for the breakdown of the hydroxide lattice are indicated.

dx.doi.org/10.1021/ic400910g | Inorg. Chem. 2013, 52, 11723−11733

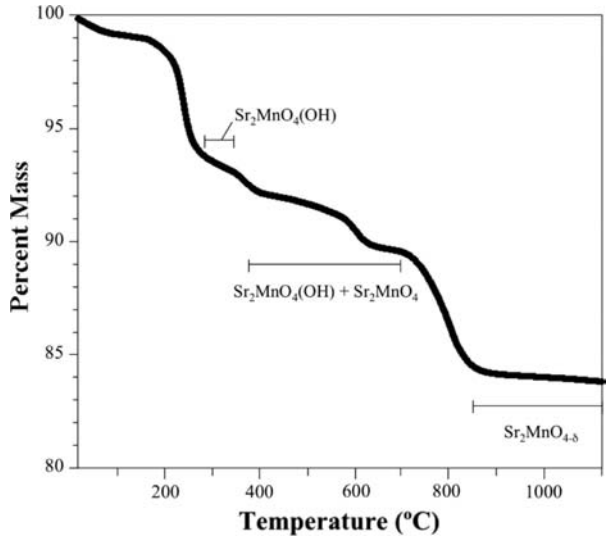

Figure 9. TGA data plot for $Sr_2Mn(OH)_6$ in air with sample compositions indicated at various temperature ranges.

changes. The final weight loss is observed between 850 and 900 °C, followed by a gradual loss all the way to 1100 °C. The decomposition product above 900 °C is pure Sr_2MnO_4 and by 1100 °C matches $Sr_2MnO_{3.615}$ reported by Gillie and coworkers.[54] TGA data corroborate this with an experimentally observed loss of mass between 150 and 1100 °C (ignoring loss of residual crystal water) of 85% versus a theoretical loss of 86.2% assuming complete conversion of the initial hydroxide to the corresponding stoichiometric oxide. Experiments performed in both air and N_2 flow yield the same product, although experiments performed in air showed the eventual thermal breakdown of $Sr_2MnO_{4-\delta}$ into $SrCO_3$ and $Sr_7Mn_4O_{15}$.[55] The previously described solid-state syntheses of Sr_2MnO_4 and $Sr_2MnO_{3.615}$ were reported to take place at 1650 and 1350 °C, respectively,[53,54] and the use of a single-source precursor significantly lowers the preparation temperature.

Analogous to the thermal decomposition of $Sr_2Mn(OH)_6$ to Sr_2MnO_4, $Ba_2Co(OH)_6$ is thermally converted to Ba_2CoO_4 under N_2 flow. This low-dimensional oxide has previously been synthesized by Boulahya and colleagues, who characterized its electronic and magnetic properties.[56] The synthesis temperature using $Ba_2Co(OH)_6$ is similar to that utilized in the solid-state synthesis previously described (900 °C), and it does not appear that a single-source precursor offers an advantage in this case. Powder X-ray diffraction analysis of the decomposition products at varying temperatures indicates that $Ba_2Co(OH)_6$ decomposes into $BaCoO_{3-\delta}$[57] and $BaCO_3$ at 375 °C instead of converting into stoichiometric products in a stepwise fashion, as is the case with $Sr_2Mn(OH)_6$.

Although no other compositions studied yielded a stoichiometric oxide product, the synthesis temperatures for some of these products are noteworthy. Some compounds are prepared at or above previously reported temperatures, such as $Ba_3Mn_2O_8$ (900 °C),[58] $BaMnO_3$ (500 °C),[59] and $BaNi_{0.85}O_{2.5}$ (1100 °C).[60] Other decomposition products are produced at temperatures lower than any previous literature report, such as $Sr_2Ni_2O_5$ (375 vs 1000 °C),[61] $Sr_6Co_5O_{15}$ (420 vs 1000 °C),[62] $BaNiO_3$ (325 vs 450 °C[63] or 600 °C[64]), $Ba_3Co_2O_6(CO_3)_{0.6}$ (525 vs 750 °C),[65] and $Sr_9Ni_{6.64}O_{21}$ (810 vs 880 °C).[66] In these cases, starting with a single-source precursor reduces diffusion distances and results in a lower preparation temperature compared to standard solid-state synthesis. However, because the precursor is nonstoichiometric with respect to the resultant oxide, alkaline-earth hydroxide or carbonate byproducts are produced. These byproducts can be washed away in most cases with dilute acid without decomposing the oxide product. The thermal decomposition of $Sr_2Co(OH)_6$ in a N_2 atmosphere yielded strontium hydroxide and an unknown product, which does not match any known pattern for an oxide containing strontium and/or cobalt. Attempts to isolate this poorly crystalline product were unsuccessful because strontium hydroxide was a major byproduct and treatment with dilute acid decomposed the oxide rapidly.

Magnetism. The temperature dependencies of the magnetic susceptibility (χ) for the nickel, cobalt, and manganese analogues, measured under zfc and fc conditions, were investigated. Temperature dependencies of the inverse susceptibility data were fit to the Curie–Weiss law $\chi = C/(T - \theta)$, where C is the Curie constant and θ is the paramagnetic Weiss temperature. All samples show purely paramagnetic behavior down to 5 K.

Because of the presence of small amounts of residual carbonate impurities, as well as potential amorphous phases such as $Ni(OH)_2$, the magnetic moments are approximate because of the uncertainty in the sample mass. $Sr_2Mn(OH)_6$ and $Ba_2Mn(OH)_6$ exhibit effective moments of 5.41 and 5.74 μ_B, respectively, which are close to that expected for Mn^{2+} (μ_{eff} = 5.92 μ_B; $S = {}^5/_2$; Figures 10 and 11). Some $Sr_2Co(OH)_6$ and

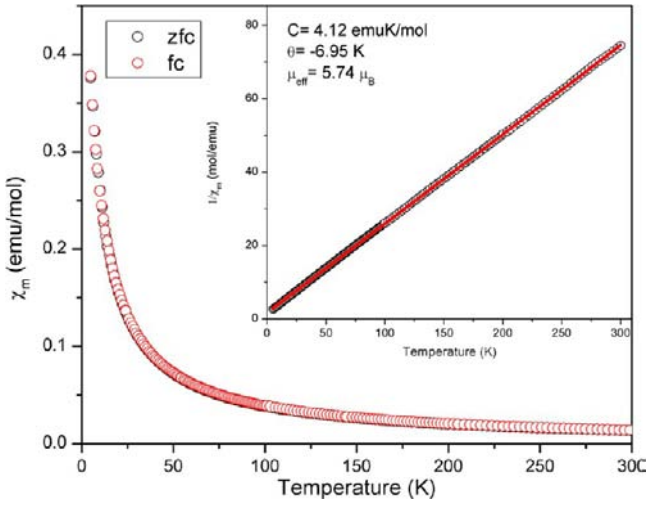

Figure 10. Temperature dependence of the molar magnetic susceptibility, χ_m, of $Sr_2Mn(OH)_6$. All measurements were carried out in an applied field of 1000 Oe. The inverse susceptibility versus temperature plot is shown in the inset with the Curie–Weiss law fit.

$Ba_2Co(OH)_6$ crystals contained small black inclusions, most likely cobalt oxide, that affected the measured moments. It was not possible to completely remove this byproduct from the synthesized crystals, and it was present in quantities too small for identification. Nonetheless, the magnetic data support strictly paramagnetic behavior for $Sr_2Co(OH)_6$ and $Ba_2Co(OH)_6$, as shown in Figures S18 and S19 in the Supporting Information, respectively. $Sr_2Ni(OH)_6$ and $Ba_2Ni(OH)_6$ also display paramagnetic behavior, and their data are shown in Figures S20 and S21 in the Supporting Information, respectively.

dx.doi.org/10.1021/ic400910g | Inorg. Chem. 2013, 52, 11723–11733

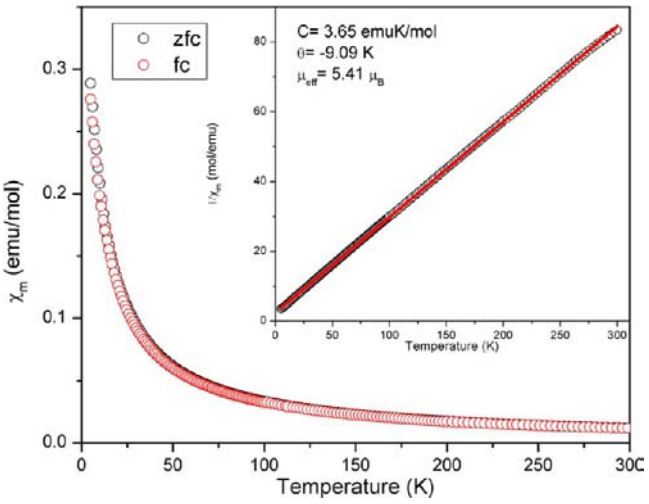

Figure 11. Temperature dependence of the molar magnetic susceptibility, χ_m, of $Ba_2Mn(OH)_6$. All measurements were carried out in an applied field of 1000 Oe. The inverse susceptibility versus temperature plot is shown in the inset with the Curie–Weiss law fit.

CONCLUSION

A series of new transition-metal hexahydroxometallates were synthesized using a hydroflux technique. $Sr_2Mn(OH)_6$, $Ba_2Mn(OH)_6$, $Sr_2Co(OH)_6$, $Ba_2Co(OH)_6$, $Sr_2Ni(OH)_6$, $Ba_2Ni(OH)_6$, and $Ba_2Cu(OH)_6$ have been prepared and structurally characterized by single-crystal X-ray diffraction. IR spectroscopy confirms the presence of and differences in the bond lengths of the three crystallographically distinct hydroxide groups. Thermal decomposition in air and nitrogen has been investigated, and the subsequent products are reported for the six new compounds. The magnetic properties of the compounds were measured, with simple paramagnetic behavior exhibited for all six hexahydroxometallates.

ASSOCIATED CONTENT

Supporting Information

X-ray crystallographic files in CIF format for all hydroxides reported, magnetic data plots for $Sr_2Co(OH)_6$, $Ba_2Co(OH)_6$, $Sr_2Ni(OH)_6$, and $Ba_2Ni(OH)_6$, and IR spectra and TGA plots for $Sr_2Mn(OH)_6$, $Ba_2Mn(OH)_6$, $Sr_2Co(OH)_6$, $Ba_2Co(OH)_6$, $Sr_2Ni(OH)_6$, and $Ba_2Ni(OH)_6$. This material is available free of charge via the Internet at http://pubs.acs.org.

AUTHOR INFORMATION

Corresponding Author

*E-mail: zurloye@mailbox.sc.edu. Tel: +1-803-777-6916. Fax: +1-803-777-8508.

Notes

The authors declare no competing financial interest.

ACKNOWLEDGMENTS

The authors gratefully acknowledge financial support from the NASA-EPSCoR program through Award 520880. The research at ORNL was supported by the U.S. Department of Energy, Basic Energy Sciences, Materials Sciences and Engineering Division. Mary Anne Fitzpatrick, Dean, and the USC selection committee are gratefully acknowledged for supporting Michael Chance via a College of Arts and Sciences Dean's Dissertation Fellowship.

REFERENCES

(1) Elwell, D.; Scheel, H. J. *Crystal Growth from High Temperature Solutions*; Academic Press: New York, 1975.
(2) Dong, Y.-B.; Smith, M. D.; zur Loye, H.-C. *Angew. Chem., Int. Ed.* **2000**, *39*, 4271.
(3) Ellsworth, J. M.; zur Loye, H.-C. *Dalton Trans.* **2008**, 5823.
(4) Férey, G.; Mellot-Draznieks, C.; Serre, C.; Millange, F.; Dutour, J.; Surblé, S.; Margiolaki, I. *Science* **2005**, *309*, 2040.
(5) Su, C.-Y.; Goforth, A. M.; Smith, M. D.; Pellechia, P. J.; zur Loye, H.-C. *J. Am. Chem. Soc.* **2004**, *126*, 3576.
(6) Zhang, W.; Ye, H.-Y.; Xiong, R.-G. *Coord. Chem. Rev.* **2009**, *253*, 2980.
(7) Aidoudi, F. H.; Byrne, P. J.; Allan, P. K.; Teat, S. J.; Lightfoot, P.; Morris, R. E. *Dalton Trans.* **2011**, *40*, 4324.
(8) Aldous, D. W.; Lightfoot, P. *J. Fluorine Chem.* **2012**, *144*, 108.
(9) Gautier, R.; Donakowski, M. D.; Poeppelmeier, K. R. *J. Solid State Chem.* **2012**, *195*, 132.
(10) Raw, A. D.; Ibers, J. A.; Poeppelmeier, K. R. *J. Solid State Chem.* **2013**, *200*, 165.
(11) Li, M.-R.; Walker, D.; Retuerto, M.; Sarkar, T.; Hadermann, J.; Stephens, P. W.; Croft, M.; Ignatov, A.; Grams, C. P.; Hemberger, J.; Nowik, I.; Halasyamani, P. S.; Tran, T. T.; Mukherjee, S.; Dasgupta, T. S.; Greenblatt, M. *Angew. Chem., Int. Ed.* **2013**, *52*, 8406.
(12) Mugavero, S. J.; Gemmill, W. R.; Roof, I. P.; zur Loye, H.-C. *J. Solid State Chem.* **2009**, *182*, 1950.
(13) Bugaris, D. E.; zur Loye, H.-C. *Angew. Chem., Int. Ed.* **2012**, *51*, 3780.
(14) Bugaris, D. E.; Smith, M. D.; zur Loye, H.-C. *Inorg. Chem.* **2013**, *52*, 3836.
(15) Scholder, R.; Felsenstein, R.; Apel, A. *Z. Anorg. Allg. Chem.* **1933**, *216*, 138.
(16) Scholder, R.; Pätsch, R. *Z. Anorg. Allg. Chem.* **1934**, *220*, 411.
(17) Scholder, R.; Hendrich, G. *Z. Anorg. Allg. Chem.* **1939**, *241*, 76.
(18) Kwestroo, W.; van Gerven, H. C. A.; van Hal, H. A. M. *Mater. Res. Bull.* **1977**, *12*, 161.
(19) Morán-Miguélez, E.; Alario-Franco, M. A.; Joubert, J. C. *Mater. Res. Bull.* **1986**, *21*, 107.
(20) Dubler, E.; Korber, P.; Oswald, H. R. *Acta Crystallogr., Sect. B* **1973**, *29*, 1929.
(21) Henning, T.; Jacobs, H. *Z. Anorg. Allg. Chem.* **1992**, *616*, 71.
(22) Hinz, D. *Z. Anorg. Allg. Chem.* **2000**, *626*, 1004.
(23) Ivanov-Emin, B. N.; Il'inets, A. M.; Zaitsev, B. E.; Kostrikin, A. V.; Spiridonov, F. M.; Dolganev, V. P. *Zh. Neorg. Khim.* **1990**, *35*, 2285.
(24) Jacobs, H.; Bock, J. *Z. Anorg. Allg. Chem.* **1987**, *546*, 33.
(25) Stahl, R.; Jacobs, H. *Z. Anorg. Allg. Chem.* **1998**, *624*, 17.
(26) Buscaglia, M. T.; Leoni, M.; Viviani, M.; Buscaglia, V.; Martinelli, A.; Testino, A.; Nanni, P. *J. Mater. Res.* **2003**, *18*, 560.
(27) Faust, G. T.; Schaller, W. T. *Z. Kristallogr.* **1971**, *124*, 116.
(28) Jacobs, H.; Stahl, R. *Z. Anorg. Allg. Chem.* **2000**, *626*, 1863.
(29) Kamaha, S.; Reuter, H. *Z. Anorg. Allg. Chem.* **2009**, *635*, 2058.
(30) Noerlund, C. A.; Hazell, R. G. *Acta Chem. Scand.* **1969**, *23*, 1219.
(31) Reuter, H.; Bargon, G. *Z. Anorg. Allg. Chem.* **1997**, *623*, 1978.
(32) Strunz, H.; Contag, B. *Acta Crystallogr.* **1960**, *13*, 601.
(33) Troyanov, S. I.; Kostrikin, A. V.; Spiridonov, F. M.; Lin'ko, I. V.; Ezhov, A. I.; Martynova, S. V.; Zaitsev, B. E. *Zh. Neorg. Khim.* **2001**, *46*, 572.
(34) Wrobel, G.; Piech, M.; Dardona, S.; Ding, Y.; Gao, P.-X. *Cryst. Growth Des.* **2009**, *9*, 4456.
(35) Yang, S.; Zavalij, P. Y.; Whittingham, M. S. *Acta Crystallogr., Sect. C* **2001**, *57*, 228.
(36) Dobson, J. V.; Taylor, M. J. *Electrochim. Acta* **1986**, *31*, 235.
(37) Dobson, J. V.; Taylor, M. J. *Electrochim. Acta* **1986**, *31*, 231.
(38) *SHELXTL*, version 6.14; Bruker Analytical X-ray Systems, Inc.: Madison, WI, 2000.
(39) *SMART*, version 5.625; *SAINT+*, version 6.45; *SADABS*, version 2.05; Bruker Analytical X-ray Systems Inc.: Madison, WI, 2001.
(40) Sheldrick, G. M. *Acta Crystallogr., Sect. A* **2008**, *64*, 112.

(41) Brown, I. D. *The Chemical Bond in Inorganic Chemistry: The Bond Valence Model*; Oxford University Press: Oxford, U.K., 2006.
(42) Sutovic, S.; Karanovic, L.; Poleti, D. *Acta Crystallogr., Sect. C* **2009**, *65*, i48.
(43) Wold, A.; Dwight, K. *Solid State Chemistry: Synthesis, Structure, and Properties of Selected Oxides and Sulfides*; Chapman & Hall: New York, 1993; pp 70−76.
(44) Vidyasagar, K.; Gopalakrishnan, J.; Rao, C. N. R. *J. Solid State Chem.* **1985**, *58*, 29.
(45) Sarkozy, R. F.; Chamberland, B. L. *Mater. Res. Bull.* **1973**, *8*, 1351.
(46) Sarkozy, R. F.; Moeller, C. W. C.; B, L. *J. Solid State Chem.* **1974**, *9*, 242.
(47) Li, G.; Feng, S.; Li, L.; Li, X.; Jin, W. *Chem. Mater.* **1997**, *9*, 2894.
(48) McLune, W. F., Ed.; Swarthmore, PA, 1989; Card No. 24-1187.
(49) Shimakawa, Y.; Jorgensen, J. D.; Mitchell, J. F.; Hunter, B. A.; Shaked, H.; Hinks, D. G.; Hitterman, R. L.; Hiroi, Z.; Takano, M. *Physica C* **1994**, *228*, 73.
(50) Nagai, I.; Kato, M.; Koike, Y. *Physica C* **2000**, *338*, 84.
(51) Scholder, R.; Schwochow, E. F. *Angew. Chem., Int. Ed.* **1966**, *5*, 1047.
(52) Baran, E. J.; Aymonino, P. J. *Monatsh. Chem.* **1969**, *100*, 1674.
(53) Bouloux, J.-C.; Soubeyroux, J.-L.; Flem, G. L.; Hagenguller, P. *J. Solid State Chem.* **1981**, *38*, 34.
(54) Gillie, L. J.; Wright, A. J.; Hadermann, J.; Van Tendeloo, G.; Greaves, C. *J. Solid State Chem.* **2002**, *167*, 145.
(55) Kriegel, R.; Feltz, A.; Walz, L.; Simon, A.; Mattausch, H. J. *Z. Anorg. Allg. Chem.* **1992**, *617*, 99.
(56) Boulahya, K.; Parras, M.; González-Calbet, J. M.; Amador, U.; Martinez, J. L.; Fernández-Díaz, M. T. *Chem. Mater.* **2006**, *18*, 3898.
(57) Zanne, M.; Courtois, A.; Gleitzer, C. *Bull. Soc. Chim. Fr.* **1972**, *12*, 4470.
(58) Weller, M. T.; Skinner, S. J. *Acta Crystallogr., Sect. C* **1999**, *55*, 154.
(59) Christensen, A. N.; Ollivier, G. *J. Solid State Chem.* **1972**, *4*, 131.
(60) Campá, J. A.; Gutiérrez-Puebla, E.; Monge, M. A.; Rasines, I.; Ruìz-Valero, C. *J. Solid State Chem.* **1994**, *108*, 230.
(61) Takeda, Y.; Hashino, T.; Miyamoto, H.; Kanamaru, F.; Kume, S.; Koizumi, M. *J. Inorg. Nucl. Chem.* **1972**, *34*, 1599.
(62) Harrison, W. T. A.; Hegwood, S. L.; Jacobson, A. J. *J. Chem. Soc., Chem. Commun.* **1995**, 1953.
(63) Lander, J. J. *Acta Crystallogr.* **1951**, *4*, 148.
(64) Krischner, H.; Torkar, K.; Kolbesen, B. O. *J. Solid State Chem.* **1971**, *3*, 349.
(65) Boulahya, K.; Amador, U.; Parras, M.; González-Calbet, J. M. *Chem. Mater.* **2000**, *12*, 966.
(66) Campá, J.; Gutirérrez-Puebla, E.; Monge, A.; Rasines, I.; Ruíz-Valero, C. *J. Solid State Chem.* **1996**, *126*, 27.